Surface-Directed Adsorption in the Epitaxy Growth of Streptocyanine Dye Crystals

Ming Li, Anfeng Wang, and Guangzhao Mao*

Department of Chemical Engineering and Materials Science, Wayne State University, 5050 Anthony Wayne Drive, Detroit, Michigan 48202

Lars Daehne

Institute of Physical Chemistry, Free University Berlin, Takustrasse 3, D-14195 Berlin, Germany

Received: August 3, 1999; In Final Form: October 5, 1999

The simple molecular structure, relatively high stability, and color variation with molecular packing structure make the streptopolymethine dyes an ideal candidate for the study of surface effects on the nucleation and growth of organic crystals at a liquid/solid interface. In situ optical and atomic force microscopy (AFM) experiments were conducted on amorphous glass and crystalline muscovite mica in order to correlate the crystal morphology and orientation with early molecular events during adsorption and nucleation. Bulk crystallization of the chloride salt of 1,7-bis(dimethylamino)heptamethinium (BDH^+Cl^-) in acetone yields prismatic crystals bound by the (001) and (110) faces. Optical study shows that, of all the substrates studied, mica has the highest selectivity toward the (001) face. The orientation of this face follows the 3-fold symmetry of the mica lattice. AFM measurements captured the early stages of BDH^+Cl^- dye crystallization on mica, such as the adsorption of single molecules, formation of rodlike aggregates, their organization into two-dimensional brickwork aggregates/crystals, and three-dimensional crystal growth. For all stages, the dye molecules were oriented edge-on along the [100] direction of the mica, yielding the (001) BDH^+Cl^- crystal face. It is concluded that BDH^+Cl^- crystallizes epitaxially on mica despite the poor match in lattice symmetry and parameters. This is realized by the weak interlayer and strong intralayer interactions and the surface-directed alignment of adsorbed BDH^+ molecules.

Introduction

More and more new electronic devices incorporate organic and polymeric materials because of their low cost, ease of synthesis, and degradability. The most interesting organic materials for electronic applications are solids of molecules having extended π-electron systems, known as dyes or chromophores. They are used widely as pigments or thin films on substrates in paints, photography, xerography, laser printers, write-once-read-many-times memory systems, color liquid crystal displays, and solar photovoltaic cells.[1] The collective properties of dye molecules, critical for these applications, often depend more on the supramolecular structure or the relative molecular arrangement, less on the molecular properties of the chromophores. This was shown recently for one of the simplest example of the cyanine dyes, the streptocyanine 1,7-bis-(dimethylamino)heptamethinium (BDH^+). BDH^+ has a simple chemical structure (Scheme 1) and known crystal structures. The highly anisotropic nature of rodlike BDH^+ molecules makes it possible to study the surface-induced orientation of adsorbed molecules and the effect of lattice symmetry mismatch.

Spin-coated crystalline films (80 nm thick) of BDH^+ exhibit unusual chameleon-like optical properties, whose color varies in the whole visible wavelength range.[2] The color variation is caused by the orientation of the dye molecules in the film as a result of three effects, namely J-aggregation, polaritons, and optical anisotropy.[3]

SCHEME 1. Chemical Structure and Electron Density Distribution of Dye Salt 1.7-bis(dimethylamino)-Heptamethine Chloride BDH^+Cl^-. Hydrogen Atoms Were Omitted in the Electron Density Calculation

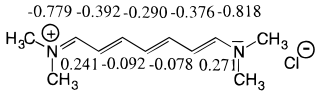

(i) The formation of J-aggregate stacks in the layer shifts the absorption to a longer wavelength with respect to that of the nonaggregated state.[4] The red shift is attributed to the slippage angle α, which is the angle between the aggregate direction and the molecular axis, according to the exciton theory.[5]

(ii) The high absorption coefficient of the BDH^+ solids[6] yields a strong polarization of the material by interaction with light. The coupling between the excitons and the polarization of the medium results in so-called polaritons. The most striking features of polaritons are the formation of a metallic reflection in crystals and a shift of absorption and reflection bands to higher energy for increasing inclination of the molecular axis with respect to the crystal face.

(iii) Furthermore, due to the optical anisotropy of this molecule, no absorption exists perpendicular to the molecule axis.

Therefore, optical investigations can provide clues to the stacking structure of the dye molecules, their inclination to the crystal plane, and their azimuthal orientation.

Assuming an epitaxy correlation between the dye molecule and the negatively charged site on mica, three stacking models

* To whom all correspondence should be addressed. Phone: (313) 577-3804. Fax: (313) 577-3810. E-mail: gzmao@chem1.eng.wayne.edu.

10.1021/jp992752p CCC: $18.00
Published on Web 11/24/1999

of J-aggregates were proposed by Kuhn et al.: the staircase, ladder, and brickwork.[7] A herringbone structure was assumed in cases where two molecular orientations exist in one unit cell.[8] Such an arrangement was found by optical luminescence investigations of 1,1′-diethylpseudoisocyanine molecules adsorbed on silver halide single crystals.[9] However, due to the distorted structure of the dye, the determination of the exact molecule orientation remains to be difficult. No direct observation of the J-aggregate molecular packing structure has been obtained in polymers, which was largely attributed to the small size of J-aggregates and packing faults or impurities.[10]

The structural manipulation of dye arrays is very important due to the influence of the supramolecular structure on their collective properties. Yet in crystal engineering, it is largely impossible to assemble a specific crystal structure from "designer" molecules due to the complicated geometry of organic molecules and the delicate balances of weak molecular forces in bulk crystals.[11] Significant progresses have been made to select stronger and specific molecular forces such as the hydrogen bonding or metal coordination to build supramolecular architecture in two- (2-D) and three-dimensions (3-D).[12] Dissimilar materials, in particularly crystalline substrates, have been used to selectively nucleate and orient crystals in epitaxial-like crystallization. The attractive interactions between a crystalline overlayer and a substrate are reinforced by a match in their lattice symmetry and dimensions.[13] Strict epitaxy warrants both the texture and the azimuthal orientation. It was shown that less than perfect one-to-one lattice point match, such as commensurism and coincidence, can also promote azimuthal orientation of organic crystals with larger lattice parameters and weaker molecular forces on inorganic substrates.[14]

The requirement of 2-D lattice match limits the types of thin films and crystals which can grow epitaxially on only a few single-crystal substrates. A new type of epitaxy, called the van der Waals epitaxy (VDWE), was found in the high quality epitaxy films of semiconductors such as $MoSe_2$ grown on S_nS_2, mica, etc., with up to 60% lattice mismatch.[15] The same type of VDWE was also observed in the Langmuir−Blodgett films of lead and manganese fatty acid salts on mica.[16] However, the molecular events leading to the azimuthal orientation in the primary layer have not been understood. Some has attributed the long range order to substrate surface defects such as dislocations.[17] To address this issue, we chose to study the crystallization of the BDH^+ dye on muscovite mica. Mica sheets can be cleaved to contain molecularly smooth planes whose lattice structure is known. BDH^+ crystals are highly anisotropic, while mica has a quasi-isotropic symmetry. Mica is stable in water and many organic solvents.

While historically the optical microscopy is the primary tool for the study of crystal growth, the atomic force microscopy (AFM)[18] represents a new generation of nanoscale surface characterization methods. It is capable of capturing events such as adsorption, diffusion, recognition, lattice reconstruction, and defect formation during crystallization at the molecular level.[19] AFM can also image small nuclei in the early stage of crystallization with a lateral resolution in angstroms and a temporal resolution in milliseconds. Here we report an in situ optical and AFM study on the heterogeneous crystallization of 1,7-bis(dimethylamino)heptamethinium dye on muscovite mica from acetone solutions. The early stages of crystallization were captured by AFM and the later stages were imaged by polarized optical microscopy.

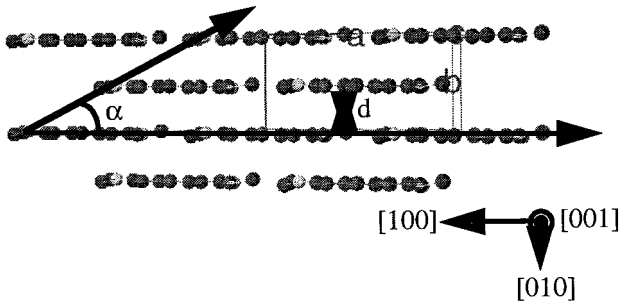

Figure 1. BDH^+Cl^- single-crystal structure according to X-ray diffraction viewed along [00$\bar{1}$] axis. The intermolecular distance d = 3.471 Å and the slippage angle α = 24.8°. The carbon atoms are represented by the dark gray spheres while the nitrogen atoms are represented by the light gray spheres. Hydrogen and chlorine atoms are omitted here.

Experimental Section

Materials. The chemical structure and electron density distribution[20] of the dye chloride salt BDH^+Cl^- are shown in Scheme 1. The positive charge is highly delocalized along the heptamethine chain. The BDH^+Cl^- was synthesized according to the literature.[21] The compound was purified extensively by alternating cycles of diethyl ether precipitation from methanol and by slow evaporation from a methanol solution including 10% water. The purity of the dye crystals was confirmed by spectroscopic methods such as UV/vis, NMR, and mass (FAB+) spectroscopies. The maximum absorption in methanol solution occurs at 510 nm with an extinction coefficient of 190000 L mol^{-1} cm^{-1}. The dye compound was kept away from light and water in order to avoid photolytic and hydrolytic degradation. HPLC grade acetone with purity > 99.7% was purchased from Fisher Scientific and used as received. The solubility of BDH^+Cl^- in acetone is 0.0023 mol/dm^3 at room temperature. Muscovite mica (grade 2, Mica New York Corp.) was cleaved just before use.

Crystal Structure and Optical Properties. The BDH^+Cl^- crystal structure belongs to the monoclinic space group C2 with lattice parameters: a = 15.248 Å, b = 6.942 Å, c = 9.074 Å, and β = 120.1°.[22] The main structural feature is the plane-parallel arrangement of dye molecules in 2-D brickwork aggregate layer (001). The BDH^+ molecule lies along the [100] direction and stacks along the [010] direction in which they are shifted by the translational operation ($^1/_2$, $^1/_2$, 0) as shown in Figure 1. The closest distance between two adjacent molecules is $d = b/2$ = 3.471 Å. The slippage angle a as shown is 24.8°. The dye molecules in adjacent layers are separated from each other by the Cl^- anions and four molecules of crystal water. There are two morphologically important faces: (001) and (110) face. The dye molecules arrange with their long edges parallel to the (001) plane, while the molecular axis is at 65.2° angle with respect to the surface normal of the (110) face. The (001) face absorbs light at 642 nm and has a mirrorlike silver reflecty. The optical images were captured by an Olympus BX60 microscope with a Sony DXC-970MD camera in transmitted light. Long-working-distance 10× objectives were used. The images were captured and analyzed by Fryer Image Pro Plus Image Analysis software with RGB capture and SVGA display hardware. The substrate was immersed in the saturated solution of the dye. As acetone slowly evaporates at room temperature the crystals were captured digitally.

Atomic Force Microscopy (AFM). Nanoscope IIIa from Digital Instruments was used. Freshly cleaved mica was mounted onto a stainless steel disk and scanned in the contact

mode at room temperature in a liquid medium. The liquid was injected through a silicone rubber tubing into a commercial fluid cell (Digital Instruments, Inc.), sealed by an O-ring. An E-scanner with a maximum scan area of $16 \times 16\ \mu m^2$ was used. The scanner was calibrated by a standard 1 μm unit length gold calibration ruling, highly oriented pyrolytic graphite (HOPG), and muscovite mica. Silicon nitride integral tips have a spring constant of 0.06 N/m and a nominal tip radius of curvature of 20−40 nm. Different scan angles were used to trace and retrace the same surface area in order to detect any tip-induced artifacts. Molecular lattices of mica and dye overlayers were captured in the deflection mode (constant height) with low gain values, while the micrometer scale images were captured in the height mode (constant deflection) with high gains. The contact force was minimized by decreasing the setpoint to just above the value which causes the detachment of the tip from the substrate surface. The molecular lattice of mica was captured before the injection of dye solutions so that the azimuthal angle between the dye overlayer and mica lattices can be obtained. Immediately after the injection of a dye solution, the surface was scanned for adsorption, nucleation, aggregation, and growth events.

Results and Discussion

First, the crystallization process of BDH^+ from acetone on amorphous glass substrates was investigated. As acetone evaporated slowly at room temperature, the incipient crystals were formed in the solution and on the acetone/air interface. Later, some crystals were found on the glass substrate surface as shown in Figure 2a. Both (001) and (110) contact planes were observed. These crystals either formed directly at the surface or gravitated onto the surface. A glass surface has no attraction toward BDH^+Cl^- and no selectivity toward any specific BDH^+Cl^- crystal faces. On the contrary, a mica surface has a strong preference toward the (001) face. Slow evaporation of acetone at room temperature yielded large crystals with perfect habit on mica as shown in Figure 2b. Only the (001) contact plane was formed as determined by the mirrorlike reflection and the face angles 50° and 130°. The orientation of the (001) face was fixed in three directions, marked numerically in Figure 2b along the long diagonal [100] axis of the BDH^+Cl^- prism. The three directions are at 60° ± 1° with respect to each other. This 3-fold symmetry indicates an azimuthal orientation of the dye crystal on mica substrate which has a hexagonal symmetry.

The evaporation rate of acetone was increased by heating the solution to 50 °C, crystals were seen to grow both on mica (Figure 2c) and at the air/acetone interface (Figure 2d). As the evaporation rate increased, the size of the crystal was reduced and its edges became more blunt due to the presence of higher energy faces. Most crystals formed on mica adopted a texture orientation of the (001) face but not an azimuthal orientation. This observation is consistent with the argument that epitaxial nucleation is less favorable as supersaturation increases.[13] A higher number of crystals were formed at the air/acetone interface. We found that surface hydrophobicity enhances the nucleation rate of BDH^+Cl^- crystallization. The crystals were also larger at the air/acetone interface due to the higher degree of molecular mobility at the liquid surface. They attached to each other to form clusters. In the extreme case of fast evaporation using the spin-coating method, where a droplet of dye acetone solution was placed on a mica substrate and the substrate was immediately spun at a rate of 3000 rpm for 5 s, needle crystals were observed due to the diffusion limited growth (Figure 2e). Three unique orientations marked numerically in Figure 2e are 60° ± 5° apart. The reflectivity gradually decreased as the light polarization rotated from the long needle axis to the perpendicular direction, which suggests that the molecular axis is along the needle axis. From the in situ optical microscopy observation, we concluded that in addition to the texture orientation of the (001) face, BDH^+Cl^- crystals also orient azimuthally on mica at near and far from equilibrium conditions.

We tried to capture the initial stages of the crystallization process by continuous scanning the mica surface in a saturated acetone solution of BDH^+Cl^- using in situ AFM. The surface was covered by adsorbed BDH^+Cl^- molecules almost immediately after the introduction of the solution. Prior to the nucleation of molecular lattices and faceted clusters, unidirectional rodlike aggregates were captured as shown in Figure 3. Reducing the scan area from $500 \times 500\ nm^2$ (Figure 3a) to $150 \times 150\ nm^2$ (Figure 3b), the individual rods (one of them marked by an arrow) is clearly visible. The rod axis was determined to parallel mica [100] axis by comparing its orientation with the orientation of the underneath mica lattice (Figure 3c) captured prior to the injection of the crystallizing medium. The misorientation angle is 3°. It shows that BDH^+ molecules displayed a high degree of orientational order before the establishment of a long-range positional order. They have a tendency to form oriented rodlike clusters, and the nucleation of BDH^+Cl^- crystals is likely assisted by these prenucleation aggregates. Absorption spectroscopy of the saturated dye solutions shows very weak aggregate absorption indicating that these aggregates were probably induced by mica substrates. It was well-known that J-aggregates prefer to form on surfaces.

Figure 4a shows a smooth surface with a uniform lattice structure captured at the beginning of crystallization. Individual BDH^+ molecules were visible as wormlike objects when the scan area was further reduced to $20 \times 20\ nm^2$ as shown in Figure 4b. By comparing the lattice orientation of bare mica (Figure 4d in the inset of Figure 4b) and the BDH^+ overlayer, it was determined that the BDH^+ molecular axis parallels a row of mica lattice points along [100] direction with a misorientation angle at most 1−2°. On the basis of the reciprocal lattice (Figure 4c in the inset of Figure 4a) from the 2-D fast Fourier transforms (fft) of the raw AFM image, we constructed a 2-D unit cell with the following parameters: $a = 15.0$ Å, $b = 6.8$ Å, and $\gamma = 99°$. The AFM data agree well with the X-ray diffraction results: $a = 15.2$ Å, $b = 6.9$ Å, and $\gamma = 90°$. The discrepancy in γ may be the result of AFM imaging distortions. We noticed that the molecule at the face center of the 2-D rectangular unit cell was missing in the AFM image. In the crystal lattice, the BDH^+ molecules are randomly rotated by 180° around the long molecule axis.[22] Therefore either the terminal methyl group or the central methine chain protrudes from the layer plane. This probably also occurs alternately in the monolayer leading to the pronounced observation of only one of the molecular sites. Limitations in the AFM lateral resolution may also account for the missing lattice molecules. It is concluded that BDH^+Cl^- molecules are highly oriented on mica, and they self-organize into a native crystal structure via the layer-by-layer growth mechanism initially. In addition, there is an azimuthal correlation between the lattice of BDH^+Cl^- overlayers and that of mica, which can be represented by BDH^+Cl^- [100]//mica[100] on BDH^+Cl^- (001)//mica(001).

Following the layer-by-layer growth, we observed the island growth mechanism. Figure 5a−c show various crystalline aggregates formation during the early stages of crystal growth.

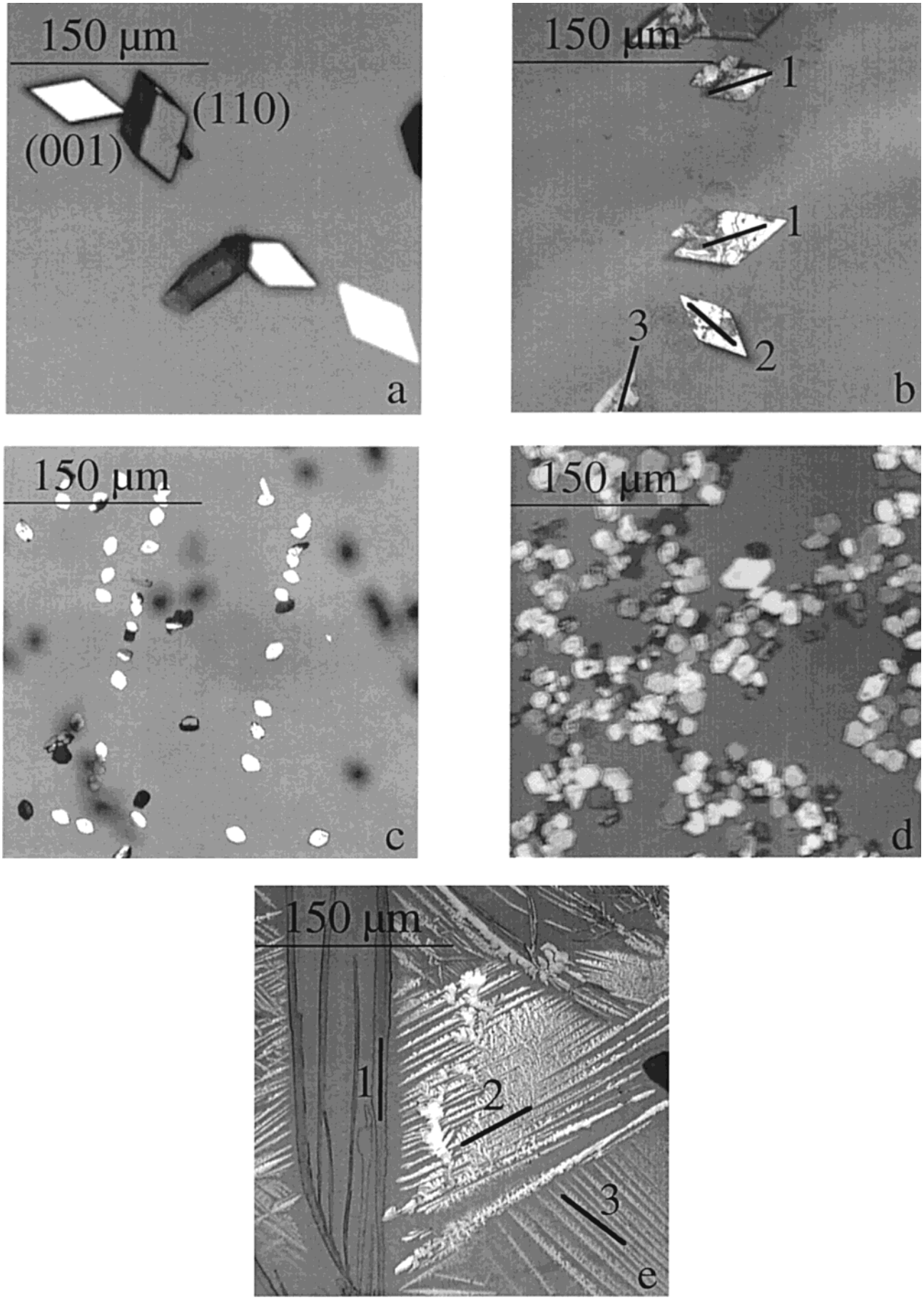

Figure 2. Optical micrographs of $BDH^{+}Cl^{-}$ crystals in the transmission mode: (a) on glass via slow evaporation at room temperature, (b) on mica via slow evaporation at room temperature, (c) on mica at 50 °C, (d) on the acetone/air surface at 50 °C, and (e) on mica via spin coating. The distinct crystal orientations are marked numerically in b and e.

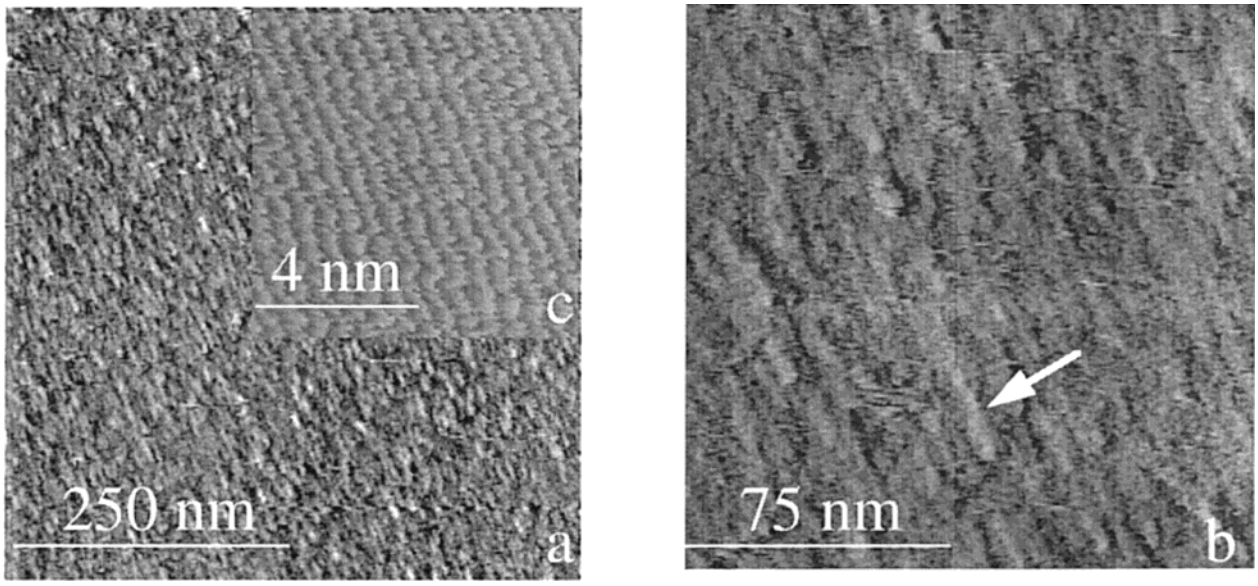

Figure 3. AFM images of BDH^+Cl^- rodlike aggregates prior to nucleation: (a) 500 × 500 nm^2 in the height mode, (b) 150 × 150 nm^2 in the height mode where the arrow points to a single rod, and (c) 8 × 8 nm^2 mica lattice underneath the aggregates in the deflection mode.

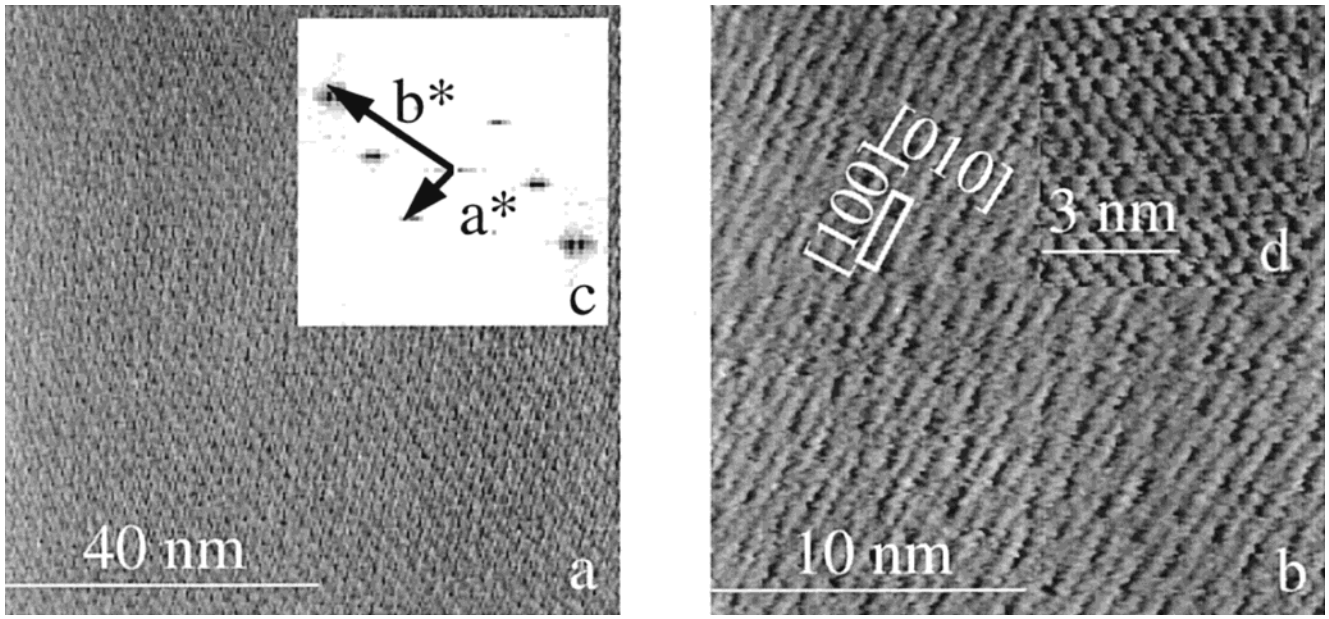

Figure 4. AFM images in the deflection mode of BDH^+Cl^- molecular lattice on mica: (a) 80 × 80 nm^2; (b) 20 × 20 nm^2 with the pseudo-rectangular unit cell resembling the surface unit cell of the (001) face, (c) the corresponding 2-D Fourier transform with a reciprocal lattice defined by a^* and b^*, and (d) 6 × 6 nm^2 mica lattice prior to nucleation.

Figure 5a and b are images of BDH^+Cl^- islands with monolayer thickness. Figure 5a is an earlier image where the islands are smaller. The islands have a uniform thickness of 5.7 ± 0.6 Å. The islands in Figure 5b are bigger with an average thickness of 8.0 ± 0.9 Å. The difference in the monolayer thickness may be the result of crystal water incorporated only at the time when Figure 5b was captured. The island does not have a well defined prismatic shape at these early stages. Figure 5b shows some islands started to adopt the characteristic shape of the mature crystal (001) face. Some islands were aligned uniformly and coalesced to form a larger assembly showing the 50° face angle of the (001) face. Figure 5c is another self-assembled pattern during the intermediate stage of crystallization. It shows BDH^+Cl^- islands coalesced to form triangles. These triangles are equilateral as the three boundaries marked numerically in Figure 5c are 60° with respect to each other. The clusters grew to multilayers indicated by their height ranging from 170 Å at the boundaries to 110 Å at the center of the triangle. In addition, the boundaries of the equilateral triangles overlap the symmetry axes of mica which implies that smaller islands attached to each other along the symmetry axis of mica. Therefore, the mica symmetry axis not only dictates BDH^+ molecular and aggregate alignment but also the attachment of the crystalline islands. These triangular patterns only existed in the intermediate stages of BDH^+ crystallization.

Theoretically there are three possible configurations for BDH^+ molecules to adsorb on a substrate surface: flat-on where the polymethine molecular plane is in contact with the substrate, edge-on where the long edge of the plane is at the substrate surface, and end-on where the short edge of the molecular plane is attached to the substrate. The electron density distribution in BDH^+ (Scheme 1) renders the central heptamethine chain more positive and the end dimethylamino group more negative. The edge-on configuration maximizes both the molecular dipole

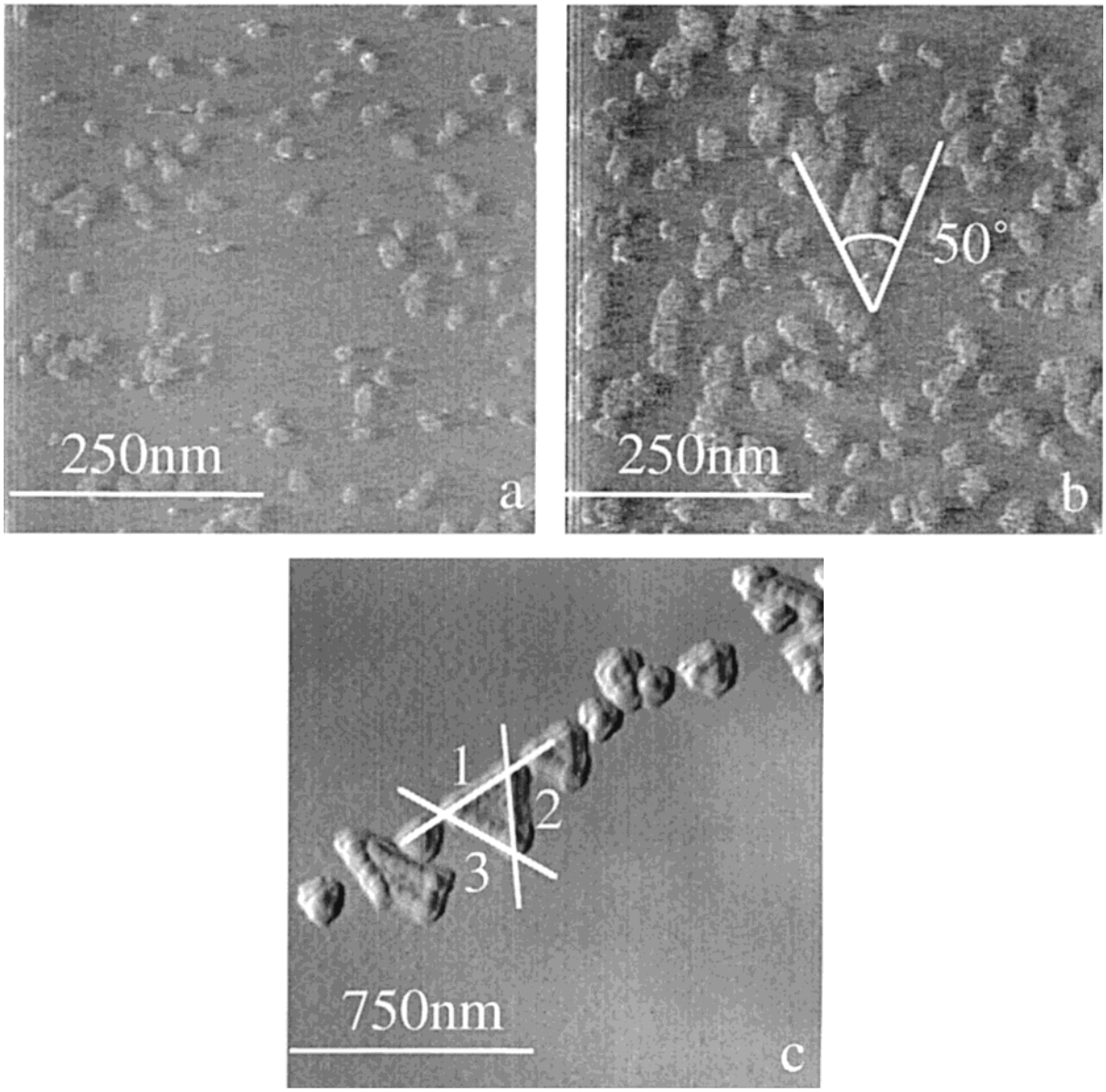

Figure 5. AFM images of BDH^+Cl^- islands. (a) Monolayer islands without crystal water in the height mode. (b) Monolayer islands with crystal water in the height mode. The emerging crystalline edges due to island coalescence resembling the (001) face are marked by white lines. (c) Multilayer islands in the deflection mode. The three specific island coalescence directions are marked numerically.

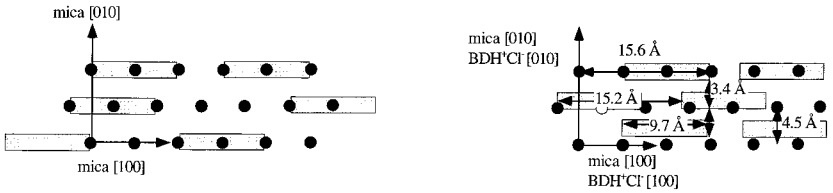

a b

Figure 6. Surface-directed adsorption and epitaxy growth: (a) molecular alignment along mica [100] axis during adsorption and (b) self-organization into the azimuthal crystalline lattice. The various spacing distances are specified in (b).

coupling between BDH^+ molecules via planar stacking, which results in J-aggregation, and electrostatic interaction with an oppositely charged and hydrophilic substrate. This explains the configuration of adsorbed BDH^+ molecules and the texture orientation of the (001) face on mica. In BDH^+Cl^- crystals, molecules stack side-by-side to form J-aggregates and an edge-on configuration is terminated at the (001) face. However, the BDH^+Cl^- (001) face and mica (001) face are different both in symmetry and lattice parameters. A coincidence condition was found when the overlayer unit cell size was allowed to relax from $a = 15.25$ to 14.94 Å, and $b = 6.94$ to 7.22 Å with γ fixed at 90° using an epitaxy calculation program.,[14,23] This coincidence requires an azimuthal angle of 14° between the [001] axes of the overlayer and mica, and a 5a × 9b overlayer supercell. However, AFM results point to an azimuthal angle of 0° between the overlayer and substrate unit cell orientations. The apparent epitaxy can be explained by a combination of several factors. First, VDWE requirement of strong intralayer

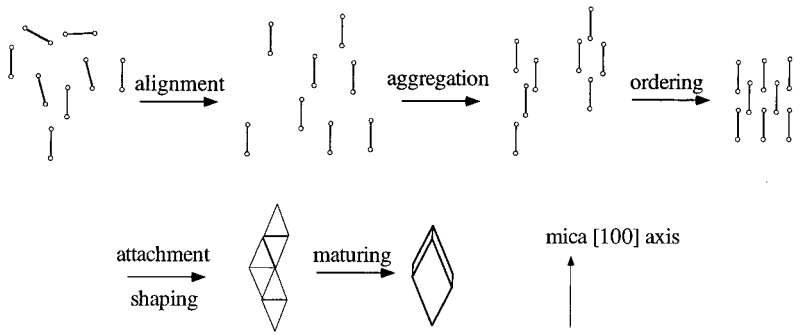

Figure 7. Proposed stepwise molecular processes in the epitaxy growth of BDH^+Cl^- crystal on muscovite mica.

and weak interlayer interactions is satisfied in this system since the dipole coupling within the crystal is much larger than the BDH^+Cl^- and mica interaction. Second, [100] axis of mica possesses the highest packing and charge density, which promotes the preferential alignment of adsorbed BDH^+ molecules as shown in Figure 6a. As the surface concentration increases, the dipole−dipole coupling between BDH^+ molecules organizes the adsorbed layer into the lattice structure of (001) as shown in Figure 6b. The azimuthal orientation may also be aided by the small lattice misfit, $(a_{BDH^+Cl^-} - 3a_{mica})/3a_{mica} = -2.6\%$.

On the basis of the microscopic study, the following nucleation and growth processes are proposed for the epitaxy growth of heptamethine crystal on muscovite mica (Figure 7). BDH^+ is attracted to the mica (001) plane because of electrostatic interaction. Flat adsorption configuration is likely at low surface concentration. To maximize the charge−charge interaction, the adsorbed BDH^+Cl^- molecules prefer to orient with their molecular axis parallel the mica symmetry axis [100]. As the surface concentration increases, the aligned molecules may switch from the flat to the edge-on configuration, so that the dipole−dipole interaction between BDH^+Cl^- molecules is possible. The dipole coupling apparently results in rodlike aggregate structure at the beginning where the long axis of the rods are parallel to the mica [100] axis. The rods display high directional order but little positional order. Due to strong dipole−dipole interactions, molecules overcome the limitation of lattice mismatch between the dye overlayer and mica, and start to organize into ordered layer structure resembling (001) face. The azimuthal crystallization has been established at this point. Subsequently, island growth mechanism dominates and molecular clusters gradually incorporate water layers and grow in all three dimensions without well-defined crystalline edges. They attach and coalesce along the symmetry axis of mica. In the end, prismatic crystals with an azimuthal orientation, which can be described by BDH^+Cl^- [100]//mica[100] on BDH^+Cl^- (001)//mica(001), are large enough to be observed by the optical microscope.

Conclusions

In situ experiments of dye crystallization were conducted on amorphous glass and crystalline muscovite mica using an optical microscope and an atomic force microscope. On the (001) cleavage plane of mica at near equilibrium growth conditions, we not only observed the preferred orientation of the (001) face, indicating an edge-on configuration of the platelike BDH^+ molecules but also the azimuthal orientation of the BDH^+ molecular axis along mica [100] axis. The same azimuthal orientation was also confirmed by the AFM images of 2-D BDH^+Cl^- molecular lattice captured in situ. AFM revealed the morphological variation in the early stages of crystallization, such as the adsorption of single molecules, the formation of one-dimensional rodlike aggregates, two-dimensional brickwork aggregates, islands of monolayer thickness corresponding to before and after the incorporation of crystal water, and patterns due to island coalescence in specific directions. Our results suggest that the weak attractions in the van der Waals epitaxy relaxed the lattice match requirement. The initiation of the epitaxy may occur during the adsorption where molecules strongly prefer a specific orientation due to molecule/substrate interactions.

Acknowledgment. Professor Mao acknowledges the Career Program of the National Science Foundation (Grant CTS-9703102) for the financial support. Dr. Daehne acknowledges the German Research Foundation and the Fond der Chemischen Industrie.

References and Notes

(1) Keller, K., Ed. Science and Technology of Photography; VCH: Weinheim, 1993. Law, K. Y. *Chem. Rev.* **1993**, *93*, 449. Wright, J. D. *Molecular Crystals*, 2nd ed.; Cambridge University Press: Cambridge, 1995. Leznoff, C. C., Lever, A. P. B., Eds. *Phthalocyanines: Properties and Applications*; VCH: New York, 1989.

(2) Dähne, L.; Reck, G.; Horvath, A.; Weiser, G. *Adv. Mater.* **1996**, *8*, 486. Daehne, L.; Tao, J.; Mao, G. *Langmuir* **1998**, *14*, 565.

(3) Tao, J.; Mao, G.; Daehne, G. *J. Am. Chem. Soc.* **1999**, *121*, 3475.

(4) Scheibe, G. *Angew. Chem.* **1937**, *50*, 212. Jelly, E. E. *Nature* **1937**, *139*, 631.

(5) Kasha, M.; McRae, E. G. *Physical Processes in Radiation Chemistry*; Augenstein, L., Ed.; Academic Press: New York, 1964; pp 23−42.

(6) Daehne, L.; Kamiya, K.; Tanaka, J. *Bull. Chem. Soc. Jpn.* **1992**, *65*, 2328.

(7) Czikkely, V.; Försterling, H. D.; Kuhn, H. *Chem. Phys. Lett.* **1970**, *6*, 11.

(8) Nolte, H. J. *Chem. Phys. Lett.* **1975**, *31*, 134.

(9) Maskasky, J. E. *Langmuir* **1991**, *7*, 407.

(10) Higgins, D.; Barbara, P. F. *J. Phys. Chem.* **1995**, *99*, 3. De Boer, S.; Vink, K. J.; Wiersma, D. A. *Chem. Phys. Lett.* **1987**, *137*, 99.

(11) Desiraju, G. Crystal Engineering: *The Design of Organic Solids* (*Materials Monograph, No. 54*); Elsevier: New York, 1989. Israelachvili, J. *Intermolecular and Surface Forces*, 2nd ed.; Academic Press: London, 1992. Whitesides, G. M.; Matthias, J. P.; Seto, C. T. *Science* **1991**, *254*, 1312.

(12) Lehn, J.-M. *Angew. Chem., Int. Ed. Engl.* **1990**, *29*, 1304. Russell, V. A.; Evans, C. C.; Li, W. U.; Ward, M. D. *Science* **1997**, *276*, 575. Als-Nielsen, J.; Jacquemain, D.; Kjaer, K.; Leveiller, F.; Lahav, M.; Leiserowitz, L. *Phys. Rep.* **1994**, *246*, 251.

(13) Gebhardt, M. *Crystal Growth: an Introduction*; Hartman, P., Ed.; North-Holland: Amsterdam, 1973; pp 105−140.

(14) Hillier, A. C.; Ward, M. D. *Phys. Rev. B.* **1996**, *54*, 14037.

(15) Koma, A.; Saiki, K.; Sato, Y. *Appl. Surf. Sci.* **1989**, *41/42*, 451. Ueno, K.; Saiki, K.; Shimada, T.; Koma, A. *J. Vac. Sci. Technol. A* **1990**, *8*, 68.

(16) Viswanathan, R.; Zasadzinski, J. A.; Schwartz, D. K. *Science* **1993**, *261*, 449.

(17) Chuchi, F. S.; Parkinson, B. A.; Ueno, K.; Koma, A. *J. Appl. Phys*. **1990**, *68*, 2168.

(18) Binnig, G.; Quate, C. F.; Gerber, Ch. *Phys. Rev. Lett.* **1986**, *12*, 930. Betzig, E.; Trautman, J. K.; Harris, T. D.; Weiner, J. S.; Kostelak, R. L. *Science* **1991**, *251*, 1468. Ulman, A. *Characterization of Organic Thin Films*; Butterworth-Heinemann: Stoneham, 1995.

(19) Schwartz, D. K.; Steinberg, S.; Israelachvili, J.; Zasadzinski, J. A. N. *Phys. Rev. Lett*. **1992**, *69*, 3354. Woodward, J. T.; Schwartz, D. K. *J. Am. Chem. Soc*. **1996**, *118*, 7861.

(20) The electron density calculations were performed using CRYSTAL 92, Calculations of Crystal Structures, Basic Set 6-21G, Ab-initio. The positive charge is carried mostly by hydrogen, which is omitted here.

(21) Nikolajewski, E.; Daehne, S. *Chem. Ber.* **1967**, *100*, 2616.

(22) Groth, P. *Acta Chem. Scand. B* **1987**, *41*, 547. Kulpe, S.; Daehne, S. *Cryst. Res. Technol*. **1987**, *22*, 375.

(23) The epitaxy calculations were performed using EPICALC program developed in Professor M. D. Ward's group, Department of Chemical Engineering and Materials Science, University of Minnesota.